Supplementary Information

Pt Single Atoms Embedded in the Ni_2P Nanocrystal Surfaces as Highly Active Catalysts for Hydrogenation of Nitriles to Primary Amines

Dehuai Liu[1], Mengjiao Huai[1], Chuanyu Si[1], Xiaocheng Lan[1,2*], Tiefeng Wang[1,2,3*]

[1]Department of Chemical Engineering, Tsinghua University, Beijing 100084, China.

[2]Ordos Lab, Ordos 017010, Inner Mongolia, China.

[3]Institute for Carbon Neutrality, Tsinghua University, Beijing 100084, China.

* Corresponding Author: Tel.: 86-10-62797490.

E-mail: lanxc@tsinghua.edu.cn; wangtf@tsinghua.edu.cn (T. F. Wang)

Table S1. Actual measurement results of Ni, P, and Pt elemental content in the catalyst using ICP.

Catalysts [a]	Ni [b]	P [b]	Pt [b]
5wt%Ni_2P/SiO_2	3.58	1.29	—
5wt%Ni_2P/SiO_2-V_P (0.05 ml)	3.24	0.89	—
5wt%Ni_2P/SiO_2-V_P (0.1 ml)	3.21	0.87	—
5wt%Ni_2P/SiO_2-V_P (0.3 ml)	3.65	0.32	—
5wt%Ni_2P/SiO_2-V_P (0.6 ml)	4.07	0.09	—
Pt(0.05wt%)-5wt%Ni_2P/SiO_2-V_P (0.05 ml)	3.25	0.92	0.028
Pt(0.05wt%)-5wt%Ni_2P/SiO_2-V_P (0.1 ml)	3.70	1.02	0.033
Pt(0.05wt%)-5wt%Ni_2P/SiO_2-V_P (0.3 ml)	3.58	0.31	0.027
Pt(0.05wt%)-5wt%Ni_2P/SiO_2-V_P (0.6 ml)	4.05	0.13	0.031
Pt(0.05wt%)-5wt%Ni_2P/SiO_2-V_P (0.1 ml)	—	—	0.029
Pt(0.1wt%)-5wt%Ni_2P/SiO_2-V_P (0.1 ml)	—	—	0.060
Pt(0.2wt%)-5wt%Ni_2P/SiO_2-V_P (0.1 ml)	—	—	0.108
Pt(0.5wt%)-5wt%Ni_2P/SiO_2-V_P (0.1 ml)	—	—	0.262

[a] The numerical values in the catalyst designation indicate the theoretical content. [b] The loading values converted to actual mass percentage (wt%).

The catalyst treated solely with the alkaline solution was denoted as Ni_2P/SiO_2-V_P (1 M, *x* mL) catalyst, whereas the catalyst synthesized using Pt precursor (20 mL, *x* wt% metal loading) and alkaline solution (1 M, *x* mL) mixture was designated as Pt_1-Ni_2P/SiO_2-V_P.

Table S2. Morphological Characteristic Parameters of the Ni_2P/SiO_2 and Pt_1-Ni_2P/SiO_2-V_P catalysts.

Catalysts	Specific surface area (m^2/g)
Ni_2P/SiO_2	190.36
Pt_1-Ni_2P/SiO_2-V_P	182.67

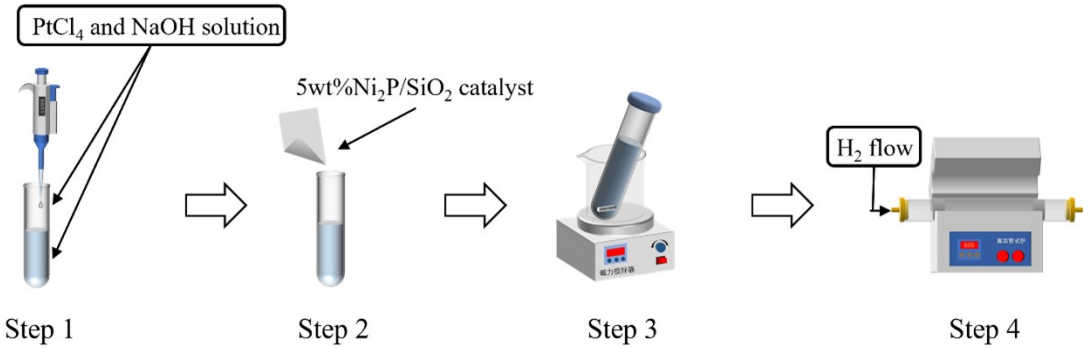

Figure S1. Catalyst's synthesis process

Step 1: Platinum (IV) tetrachloride [$PtCl_4$, 98%] and sodium hydroxide [NaOH, 96%] solutions were slowly added dropwise into deionized water to prepare an alkaline Pt precursor solution.

Step 2: 0.2 g of 5wt% Ni_2P/SiO_2 catalyst was added to the pre-prepared alkaline Pt precursor solution.

Step 3: The mixed solution was magnetically stirred for 12 h, ultrasonicated for 1 h, and then separated using a high-speed centrifuge to obtain the solid sample. The obtained solid sample was dried overnight in an oven at 60°C and briefly ground using a mortar.

Step4: The sample in step 3 was reduced at 500℃ for 2 h with a hydrogen flow of 50 ml/min. In this step, the oxide species were reduced to form the Pt_1-$Ni^{\delta+}$ pair sites.

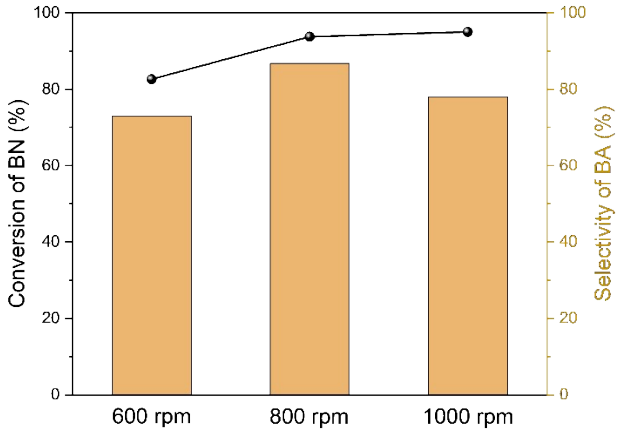

Figure S2. The evaluation results of the catalytic performance of Ni_2P/SiO_2 for benzonitrile (BN) hydrogenation under different stirring speeds (measured at 8 h).

To eliminate the influence of external mass transfer limitations on the reaction rate during the catalytic process, we investigated the conversion of benzonitrile (BN) and selectivity toward benzylamine (BA) over the Ni_2P/SiO_2 catalyst after 8 h of reaction under different stirring speeds. The results showed that the BN conversions at 800 rpm and 1000 rpm were comparable after 8 h of reaction, indicating that a stirring rate of 800 rpm is sufficient to overcome external diffusion limitations, thereby ensuring an intrinsic evaluation of the catalytic performance.

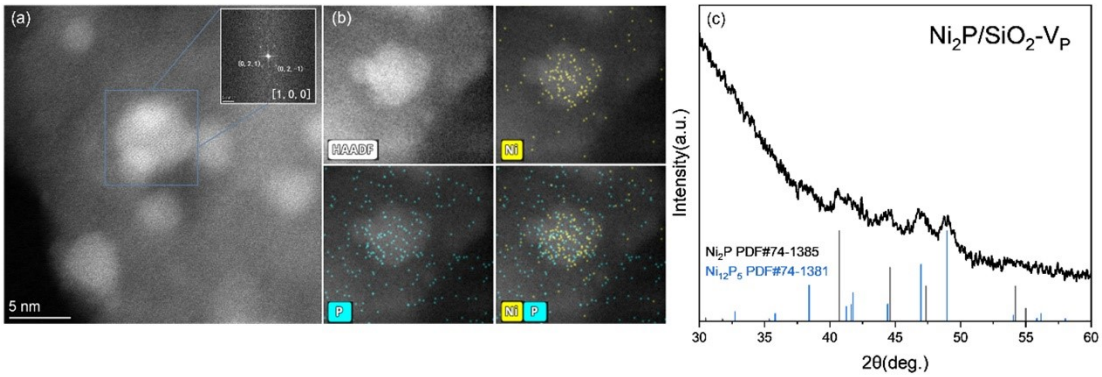

Figure S3. (a) The HAADF-STEM image of Ni_2P/SiO_2-V_P. **(b)** The EDX images of Ni_2P/SiO_2-V_P, Ni, P are shown in yellow and cyan, respectively. **(c)** The XRD patterns of Ni_2P/SiO_2-V_P.

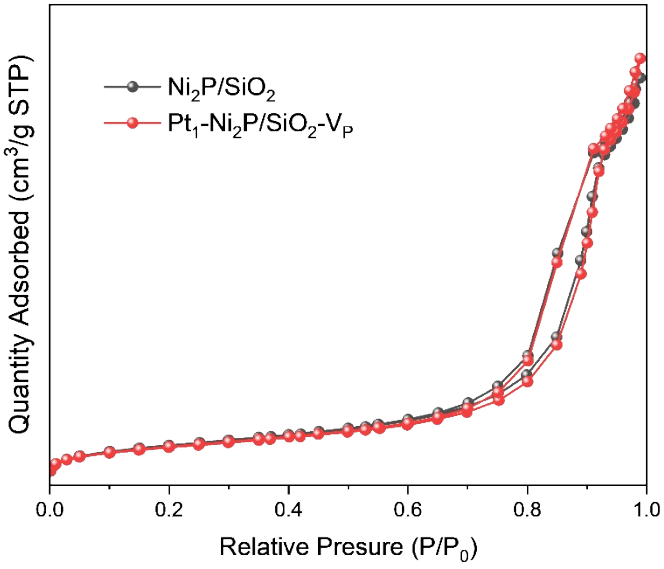

Figure S4. N_2 physisorption isotherm curves of the Ni_2P/SiO_2 and Pt_1-Ni_2P/SiO_2-V_P catalysts.

Characterized the pore structures of the Ni_2P/SiO_2 and Pt_1-Ni_2P/SiO_2-V_P catalysts using N_2 adsorption–desorption isotherms. The experimental results show that, within the experimental error, the two catalysts exhibit identical pore structure characteristics (pore volume and pore size distribution), as well as comparable specific surface areas (Table S2). This indicates that the alkali etching method does not affect the intrinsic catalytic activity by altering the specific surface area of the catalyst.

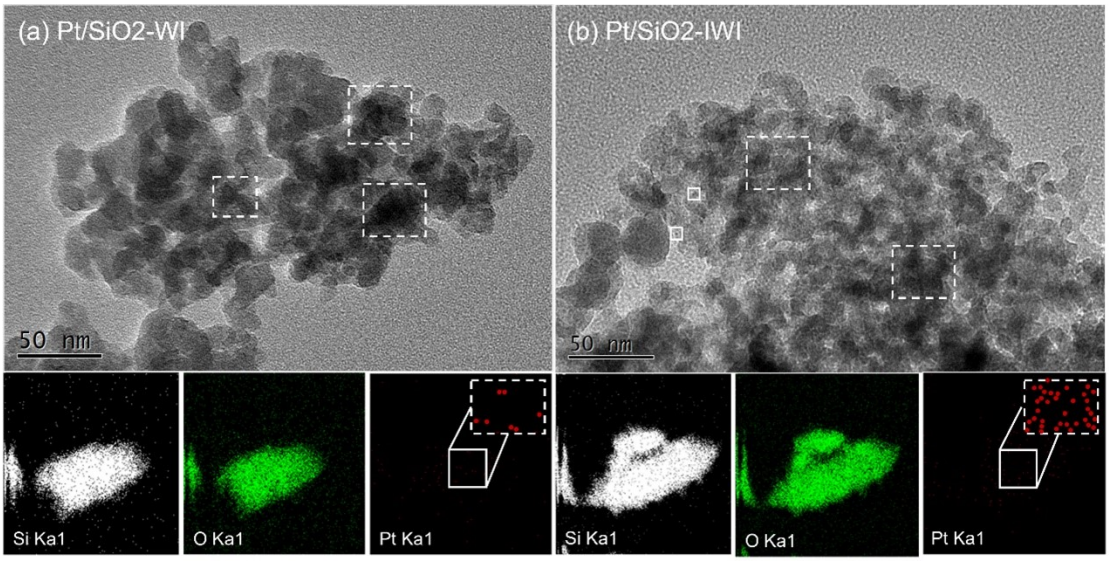

Figure S5. The TEM and EDS images of (a) 0.05wt% Pt/SiO_2-EXIM, (b) 0.05wt% Pt/SiO_2-EVIM.

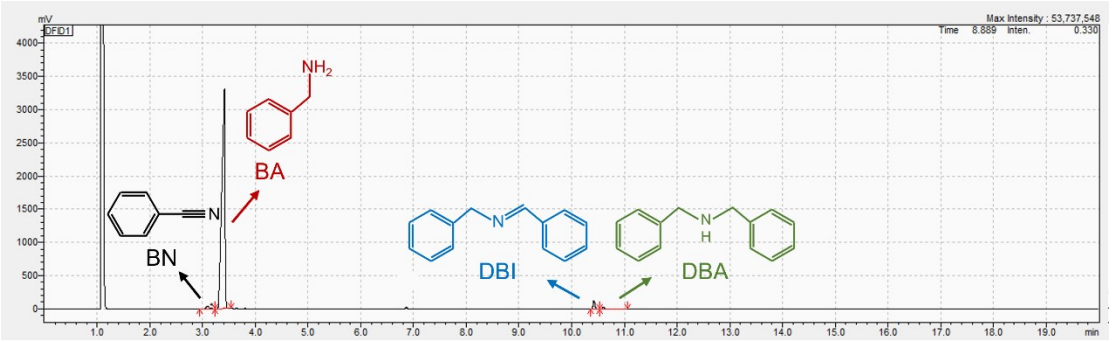

Figure S6. Chromatogram obtained after a reaction over the Pt_1-Ni_2P/SiO_2-V_P catalyst.

To track the evolution of intermediates and by-products, we have supplemented the typical chromatogram of the reaction system for clarification. Throughout the reaction process, four species can be consistently detected: BN, BA, DBI, and DBA. Regarding the imine intermediate (BI), it is highly unstable under the reaction conditions and is readily hydrogenated to BA. As a result, BI is rarely detected in the product analysis. BI predominantly exists as a surface-adsorbed intermediate on the catalyst active sites rather than as a stable free species in the reaction medium. For the deamination by-product toluene (TOL), it was not observed in our system. This is consistent with literature reports indicating that TOL formation typically occurs under harsher conditions, such as higher temperatures in gas-phase reactions, rather than under the present mild liquid-phase conditions. Given that BA is the target product and the amounts of by-products (DBI and DBA) are relatively minor, our main discussion has focused on the concentration profile of BA.

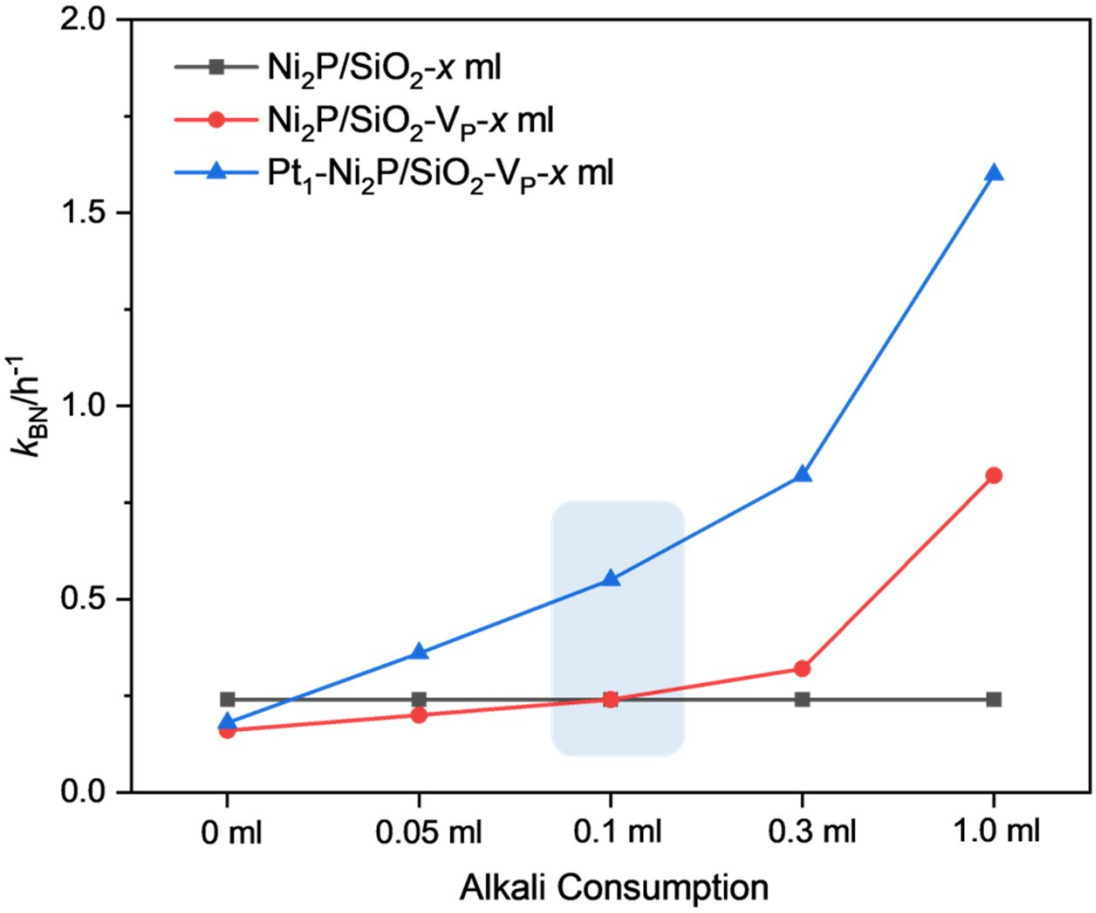

Figure S7. Comparison of reaction performance of Ni_2P/SiO_2, Ni_2P/SiO_2-V_P, and Pt_1-Ni_2P/SiO_2-V_P catalysts under varying alkaline treatment conditions.

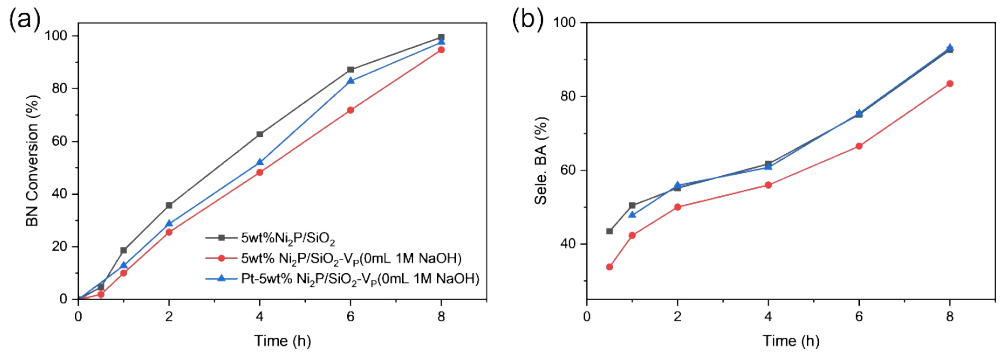

Figure S8. Catalytic performance of benzonitrile hydrogenation without P vacancies for Pt atom anchoring.

Ni_2P/SiO_2 without alkali-assisted P vacancy construction was subjected to the same Pt embedding treatment. The results show that the hydrogenation activity remains almost unchanged compared with pristine Ni_2P/SiO_2, indicating that Pt_1-$Ni^{\delta+}$ pair sites are not formed in the absence of P vacancies.

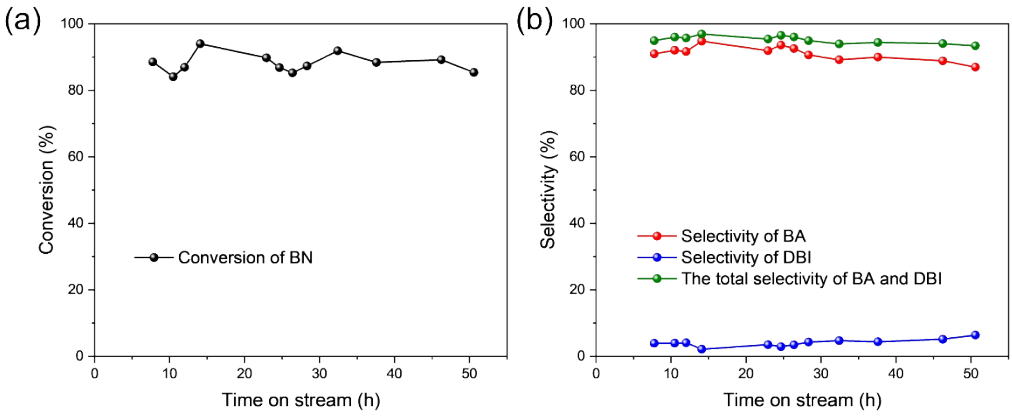

Figure S9. The long-term stability evaluation of Pt_1-Ni_2P/SiO_2-V_P was carried out by monitoring both the (a) BN conversion and (b) BA selectivity.

The long-term stability of the Pt_1-Ni_2P/SiO_2-V_P catalyst was evaluated in a trickle-bed reactor with an inner diameter of 8 mm. The concentration of benzonitrile in the feedstock was the same as that used in the batch reactor. The NH_3 concentration was 3.5 mmol/mL, and the liquid hourly space velocity (LHSV) was set to 0.02 mL/mg_{cat}/h. The reaction temperature was maintained at 130 °C, with a H_2 pressure of 4 MPa and a H_2 flow rate of 20 mL/min. Samples were periodically withdrawn from the sampling port and analyzed using gas chromatography under conditions consistent with those employed in the batch reactor.

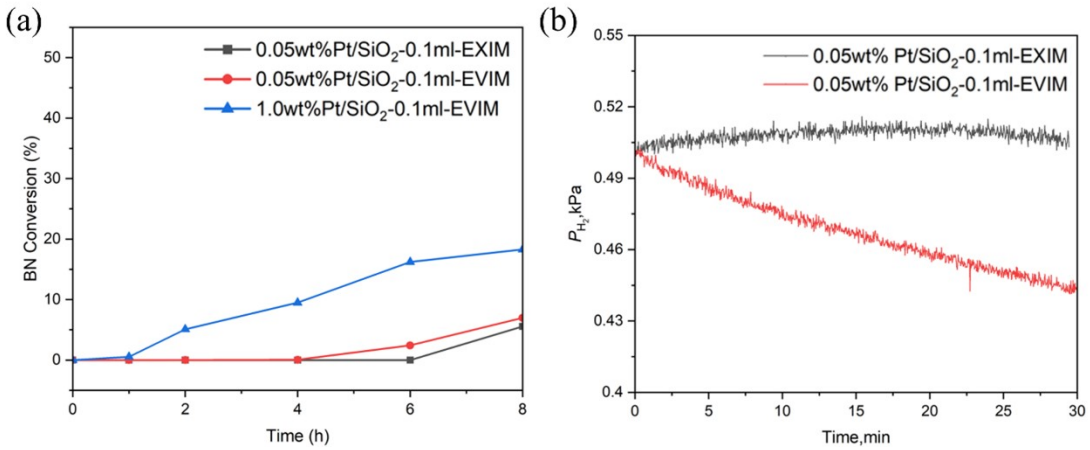

Figure S10. (a) Catalytic activity of the catalysts for BN selective hydrogenation. **(b)** H_2 partial pressure versus reaction time during the H_2-D_2 exchange reaction over the three catalysts, where the reaction rate constant (k_{HD}) was fitted based on initial data of P_{H_2}.

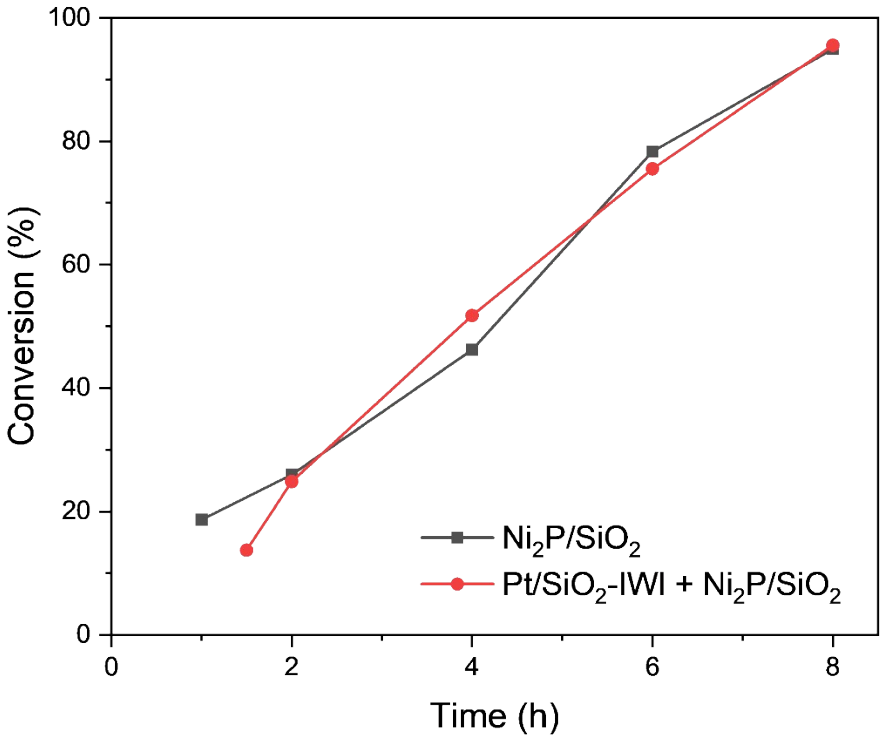

Figure S11. The reaction performance of the physical mixing experiment of Pt/SiO_2-IWI and Ni_2P/SiO_2.

To further demonstrate that the enhanced catalytic performance of the Pt_1-Ni_2P/SiO_2-

V_P catalyst for the hydrogenation of benzonitrile originates from the synergistic site effect arising from the atomic-scale proximity between Pt and $Ni^{\delta+}$, we physically mixed 25 mg of Pt/SiO_2-IWI catalyst with 25 mg of Ni_2P/SiO_2 catalyst and evaluated the catalytic activity under identical reaction conditions. The activity was found to be comparable to that of Ni_2P/SiO_2 alone (25 mg), demonstrating that the synergistic site effect arising from the atomic-scale proximity between Pt and $Ni^{\delta+}$ is the primary reason for the enhanced catalytic performance.

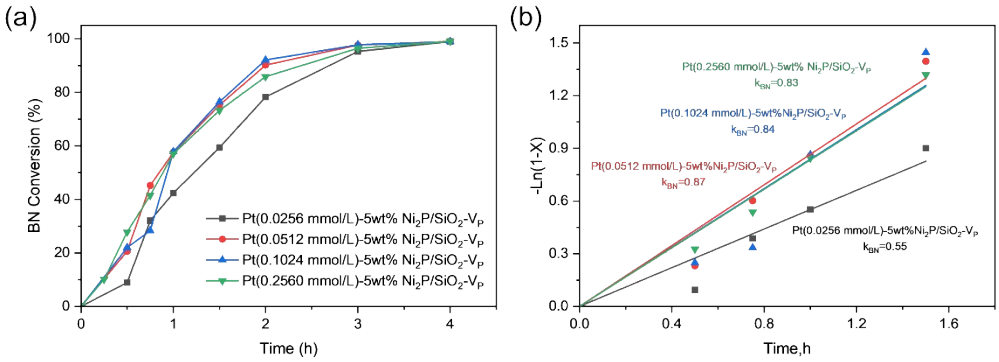

Figure S12. Catalytic performance of the Pt-Ni_2P/SiO_2-V_P treated with varying Pt precursor concentrations. (a) Catalytic activity of the catalysts for BN selective hydrogenation. (b) The reaction rate constant (k_{BN}) was fitted based on the first-order kinetics for prepared catalysts.

Ni_2P/SiO_2-V_P, prepared via alkali-assisted chemical etching, was treated with Pt precursor solutions of varying concentrations. The results show that when the concentration of the Pt precursor solution exceeds 0.0256 mmol/L, the catalytic activity remains nearly unchanged. This observation indicates that increasing Pt loading beyond a certain threshold does not lead to the formation of additional Pt_1-$Ni^{\delta+}$ active sites when the concentration of P vacancies is fixed. In other words, the number of active Pt sites is limited by the available P vacancies. This behavior strongly suggests that Pt atoms preferentially anchor at these vacancy sites, and that such sites act as the exclusive anchoring centers.

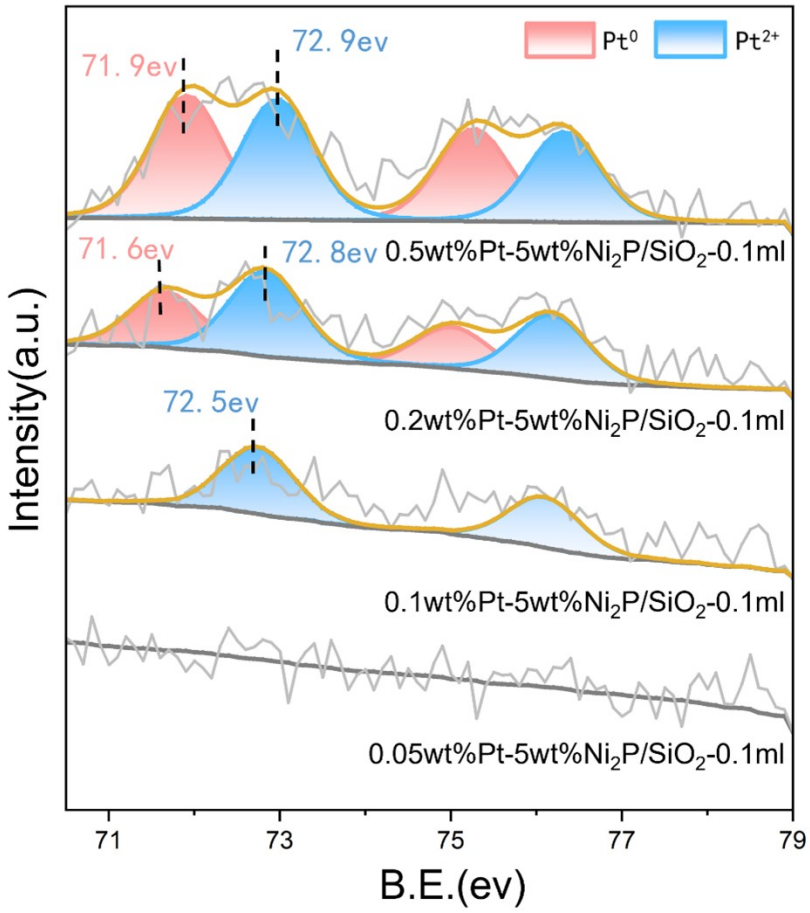

Figure S13. Surface active sites identification over the catalysts. The XPS spectra of P 2p.

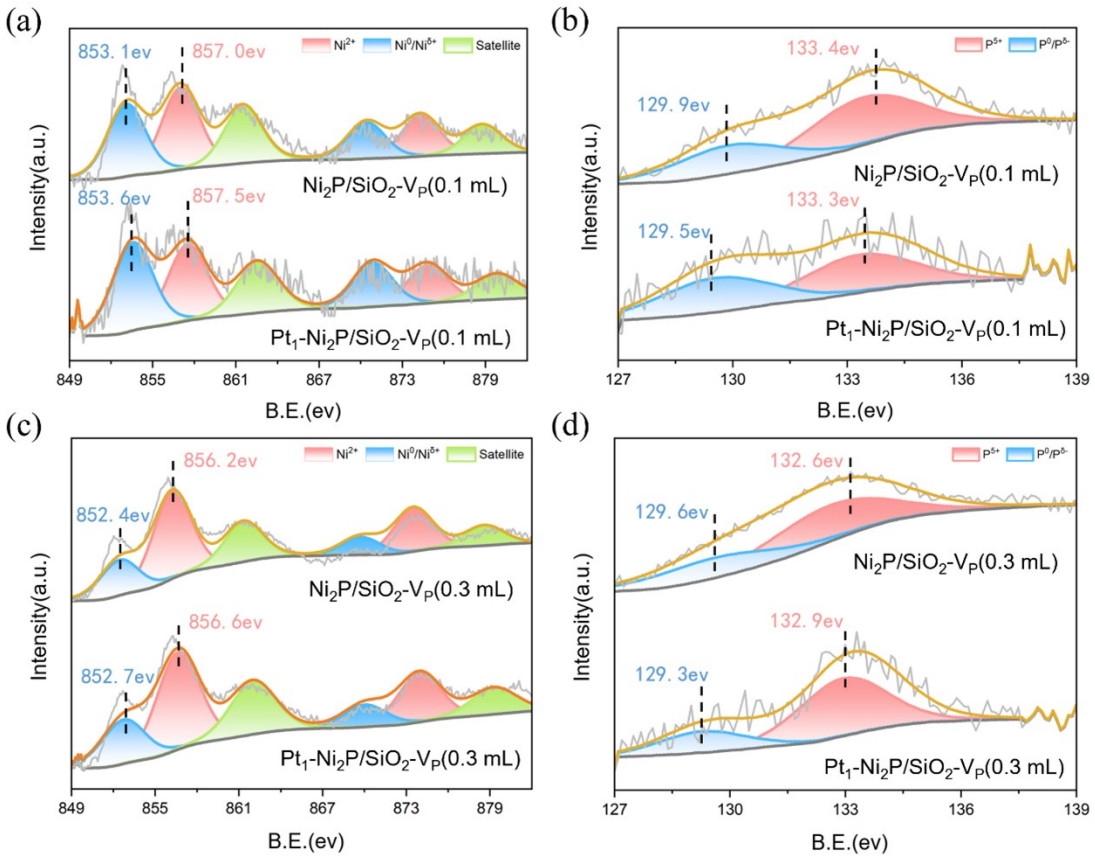

Figure S14. Surface active sites identification over the catalysts. The XPS spectra of **(a) (c)** Ni 2p, **(b) (d)** P 2p.

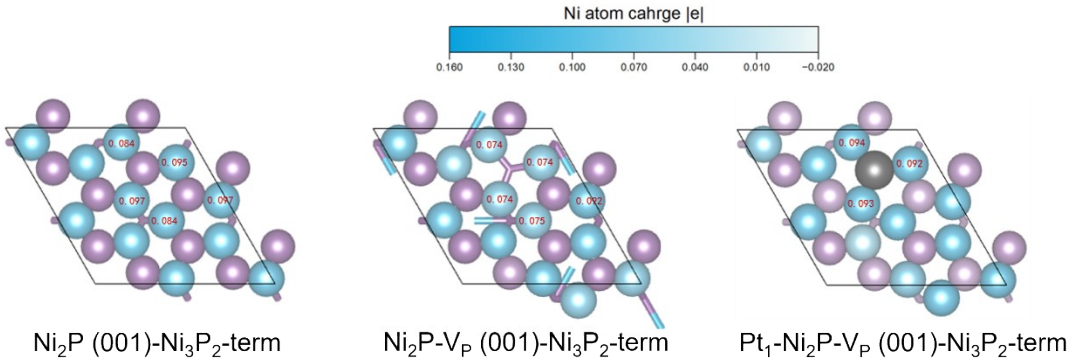

Figure S15. Bader charge analysis of the Ni_2P (001)-Ni_3P_2-term surface.

Density Functional Theory Calculations. The complex structures of Ni phosphides lead to several potential exposed surfaces make DFT calculations difficult. Theoretical calculations in previous work indicated that Ni_2P (001) have the lower surface formation energies and P-rich termination surfaces such as Ni_2P (001)-Ni_3P_2 were found to be more stable, most computational studies examine these determine. We used a surface slab model which contained 12 Ni and 8 P atoms per unit cell. Then constructed P vacancies on the surface and subsequently filled Pt atoms into these vacancies. During this process, we monitored the changes in the Bader charge of Ni atoms surrounding the P vacancies. The computational results show that after the construction of P vacancies alone, the Bader charge values of the surrounding Ni atoms decrease. Upon further filling with Pt atoms, the Bader charge values of the Ni atoms increase, indicating that surface charge is transferred from the surrounding Ni atoms to the Pt atom.